
ADAMANIP: ADAPTIVE ARTICULATED OBJECT MANIPULATION ENVIRONMENTS AND POLICY LEARNING

Anonymous authors

Paper under double-blind review

ABSTRACT

Articulated object manipulation is a critical capability for robots to perform various tasks in real-world scenarios. Composed of multiple parts connected by joints, articulated objects are endowed with diverse functional mechanisms through complex relative motions. For example, a safe consists of a door, a handle, and a lock, where the door can only be opened when the latch is unlocked. The internal structure, such as the state of a lock or joint angle constraints, cannot be directly observed from visual observation. Consequently, successful manipulation of these objects requires adaptive adjustment based on trial and error rather than a one-time visual inference. However, previous datasets and simulation environments for articulated objects have primarily focused on simple manipulation mechanisms where the complete manipulation process can be inferred from the object’s appearance. To enhance the diversity and complexity of adaptive manipulation mechanisms, we build a novel articulated object manipulation environment and equip it with 9 categories of articulated objects. Based on the environment and objects, we further propose an adaptive demonstration collection pipeline and a 3D visual diffusion-based imitation learning that learns the adaptive manipulation policy. The effectiveness of our designs and proposed method are validated through both simulation and real-world experiments.

1 INTRODUCTION

Among the various categories of objects in our daily life, articulated objects are highly significant as they are common in our surroundings (such as cabinets, doors, and laptops) and complicated for the parts with rich and diverse geometries, semantics, articulations, and functions. Therefore, learning articulated object representation (Du et al., 2023; Wei et al., 2022; Heppert et al., 2023; Lei et al., 2024) and manipulation (Xu et al., 2022; Wu et al., 2022) are essential while challenging for future robots in home-assistant tasks.

Among articulated object manipulation tasks, door manipulation (Urakami et al., 2019) is first and most thoroughly studied, as doors are most common and useful in our daily lives. Afterwards, with the release of diverse articulated object manipulation datasets and environments (Mo et al., 2019; Xiang et al., 2020; Liu et al., 2022; Geng et al., 2023b), various manipulation tasks (like opening, sliding, rotating, and further language-guided manipulation) on many categories of articulated objects (such as pots, lamps, and cabinets) have been studied.

While previous covered various aspects of articulated object manipulation, one of the most essential features of articulated objects, the mechanisms of different parts and articulations for accomplishing the final manipulation goal, has yet to be explored. For example, a safe can be directly opened by pulling the door in previous environments, while in the real world, the robot may first turn the key to unlock the door, and then pull open the door. While UniDoorManip (Li et al., 2024b) proposes an environment with the corresponding dataset that can simulate the mechanisms of doors, the mechanisms of various types of articulated objects could be much more diverse and complicated. Therefore, we build an environment that can simulate the above-described complex mechanisms of articulated object manipulation, equipping this environment with 9 categories of different objects covering 5 types of adaptive mechanisms (details described in Section 3).

The different mechanisms of articulated objects call for two core capabilities of the policy: (1) multi-modal action proposal and (2) adaptive manipulation from history actions. For an observed

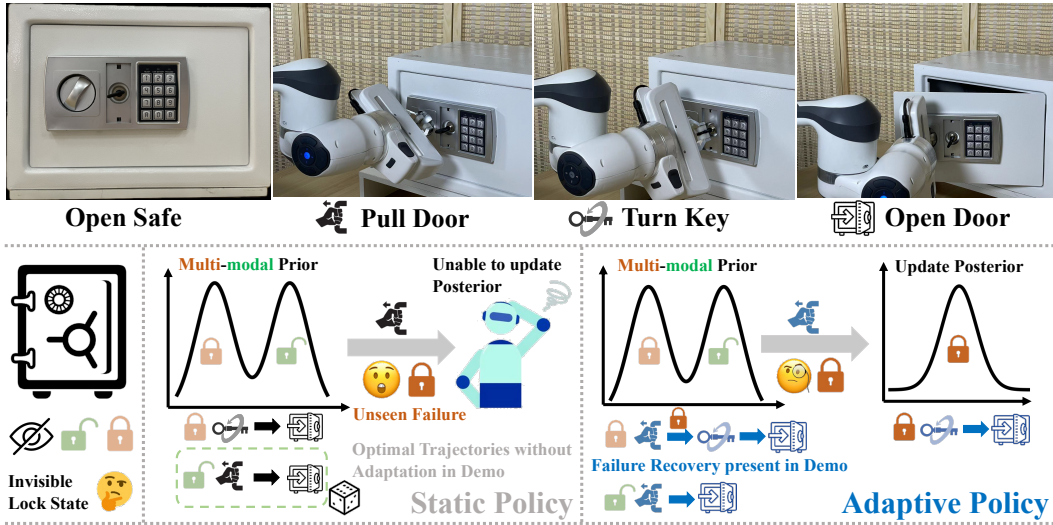


Figure 1: Example comparison between **Static** and **Adaptive Policies**. The safe can be directly opened if unlocked; otherwise, the key must be turned to unlock the latch before opening the door. However, it is impossible to figure out the lock state from pure visual observations. **Static Policy**: The demonstrations for training the static policy are optimal trajectories under full observation, including both locked and unlocked states. Consequently, the learned policy is a bimodal distribution based on visual observation alone. If the robot samples the "unlocked trajectory" and fails to open the locked door, it will be out of distribution. **Adaptive Policy**: The demonstrations for training the adaptive policy include recovery from the failed door opening. Therefore, the policy learns to first pull the door to check the lock state and updates the policy distribution accordingly based on the feedback.

object, the manipulation policy contains multiple modes, which may include different manipulation methods. For example, when observing the safe with its door closed (Bottom-Left in Figure 1), to achieve the goal of opening the door, the policy could be either directly pulling the door (when the door is unlocked) or turning the key and then pulling the door (when the door is locked), and the method should be able to model these modalities from the same visual observation (Bottom-Middle in Figure 1).

Further, to figure out and execute the accurate action from the multi-modal manipulation action candidates require adapting the manipulation policy from the history actions with their corresponding results. For example, when pulling the door and finding the door unmoved, the policy should adapt from proposing multi-modal actions (either pulling the door or turning the key) to single-modal action (turning the key) (Bottom-Right in Figure 1).

To support multi-modal action proposals, we take advantage of the designs of diffusion policy (Chi et al., 2023) and its following studies (Ze et al., 2024; Yan et al., 2024), which have demonstrated modeling multi-modal distributions from only a few successful demonstrations. To empower the policy with adaptive manipulation abilities, while previous studies only employ optimal success trajectories (without any failures during the manipulation) for training, we introduce trajectories, including failure actions and the recovery and adaptation actions from failures for training, as the failure actions help in revealing the accurate mechanisms and manipulation policy. Figure 1 showcases the superiority of our proposed adaptive policy learning method. The pure visual observation could not tell whether the door was locked or not. The static policy that only takes the passive one-frame visual input will randomly propose one of the multi-modal trajectory candidates. On the contrary, the adaptive policy will first try pulling the door, and then adapt the policy distribution from multi-modal to single-modal accordingly, as its training data include the failure of a direct pulling trial on the locked safe door, and then adaptively turning the key to open the safe after the failure successfully.

Based on our proposed novel environment, we have conducted extensive experiments on 9 categories of 277 different objects, covering 5 types of mechanisms, showcasing the necessity of the proposed environment and dataset, and the effectiveness of the proposed policy learning framework in efficiently and intelligently adapting the manipulation.

108 In summary, our contributions include:

- 109 • We study the novel problem of adaptively manipulating articulated objects with diverse
- 110 mechanisms and build an environment with various categories of objects and mechanisms.
- 111 • We propose a novel framework that learns the adaptive manipulation policy for various
- 112 mechanisms from diverse demonstrations.
- 113 • Extensive experiments have demonstrated the significance of our proposed environment,
- 114 and the effectiveness of the proposed adaptive policy learning framework.
- 115
- 116

117 2 RELATED WORK

118 2.1 ARTICULATED OBJECT ENVIRONMENTS AND DATASETS

119 To facilitate the study of representation and manipulation of diverse and complex articulated ob-
120 jects, DoorGym (Urakami et al., 2019), the door manipulation environment is first introduced with
121 diverse doors. UniDoorManip (Li et al., 2024b) further empowers door environments with different
122 mechanisms. PartNet-Mobility dataset first introduces multiple categories of articulated objects from
123 PartNet (Mo et al., 2019; Chang et al., 2015), equipped by the sapien environment (Xiang et al.,
124 2020; Mu et al., 2021; Gu et al., 2023) to support various articulated object manipulation tasks.
125 Further, GPartNet (Geng et al., 2023b) provides fine-grained part annotations, AKB-48 (Liu et al.,
126 2022) provides real-world articulated object models, and Arnold (Gong et al., 2023) provides the
127 environment for language-guided manipulation.

128 2.2 ARTICULATED OBJECT MANIPULATION

129 There have been a series of studies studying articulated object manipulation. Where2Act (Mo et al.,
130 2021) first studies the point-level affordance for short-term manipulation, with affordance-based (Wu
131 et al., 2022), flow-based (Eisner et al., 2022; Zhang et al., 2023), part-based (Geng et al., 2023a) and
132 rl-based (Geng et al., 2023c) methods study the long-horizon manipulation. Environment-Aware
133 Affordance (Wu et al., 2023a; Li et al., 2024a) further studies the manipulation with environment
134 constraints. Where2Explore (Ning et al., 2023) and AdaAfford (Wang et al., 2022) further convert
135 passive visual priors to manipulation posteriors using the few-shot interactions, respectively, tackle
136 the problem of exploring novel articulated object categories with novel geometries and parts, and
137 manipulation on ambiguous kinematics and dynamics. Besides, coarse-to-fine method (Ling et al.,
138 2024) studies the sim2real framework for real-world manipulation, and language-guided methods (Xu
139 et al., 2024; Gong et al., 2023) study the manipulation with language guidance. While these works
140 usually only studied the manipulation with simple mechanisms (such as directly opening a door or
141 safe), in our work, we further study the policy for manipulating articulated objects with diverse and
142 complex mechanisms, with a novel proposed environment supporting such objects.

143 3 ADAPTIVE MANIPULATION ENVIRONMENT

144 Previous datasets and simulation environments for articulated objects often lack diversity and realistic
145 manipulation mechanisms (Urakami et al., 2019; Li et al., 2024b; Geng et al., 2023b; Xiang et al.,
146 2020; Geng et al., 2023a). To address this issue, we developed a new environment to explore complex
147 mechanisms in articulated object manipulation better and learn adaptive manipulation policies. Based
148 on IsaacGym (Makoviychuk et al., 2021), this environment simulates these mechanisms and includes
149 9 categories of objects (Section 3.1) with 5 types of adaptive mechanisms (Section 3.2).

150 3.1 ARTICULATED OBJECT DATASET

151 In recent years, several works have proposed datasets for articulated object manipulation. PartNet-
152 Mobility (Xiang et al., 2020) and AKB-48 (Liu et al., 2022) offer diverse datasets for articulated
153 objects but focus on cross-category geometry diversity, neglecting the mechanisms of different parts
154 and articulations needed to achieve the final manipulation goal. For instance, PartNet-Mobility
155 includes the safe category, but the door can be directly opened without rotating the knob to unlock
156 the latch. GPartNet (Geng et al., 2023b) provides fine-grained part annotations but still fails

Table 1: Statistics of our adaptive articulated object dataset, including 9 categories of 277 different instances. **CM**, **PC**, respectively denote Coffee Maker and Pressure Cooker.

Category	Bottle	Pen	CM	Window	Door	Lamp	Microwave	Safe	PC
Instance	32	36	18	30	57	25	37	36	6

Table 2: Adaptive manipulation mechanism comparison between our environment and others.

Environment	Lock	\pm Clockwise	Rotate&Slide	Push/Rotate	Switch Contact
GAPartNet	\times	\times	\times	\times	\times
PartManip	\checkmark	\times	\times	\times	\times
DoorGym	\checkmark	\times	\times	\times	\times
UniDoorManip	\checkmark	\checkmark	\times	\times	\times
Ours	\checkmark	\checkmark	\checkmark	\checkmark	\checkmark

to model complex manipulation mechanisms. DoorGym (Urakami et al., 2019) claims a large-scale, scalable dataset specifically for door manipulation, considering the latch mechanism of doors. UniDoorManip (Li et al., 2024b) enriches the diversity of door geometry by composing instances. However, both DoorGym and UniDoorManip are limited to door manipulation and do not cover more diverse and long-term mechanisms.

To investigate real-world articulated object manipulation, we introduce a new dataset that encompasses more realistic adaptive manipulation mechanisms. Our dataset includes 9 categories of 277 objects: **Bottle**, **Pen**, **Coffee Maker**, **Window**, **Pressure Cooker**, **Lamp**, **Door**, **Safe**, and **Microwave**. Table 1 provides detailed statistics of our dataset, and Figure 2 visualizes instances of each category. **The object assets in our dataset are handcrafted from materials primarily obtained from 3D Warehouse (Trimble). More details can be found in Appendix B.**

3.2 ADAPTIVE MANIPULATION MECHANISM

Most existing articulated object environments focus primarily on geometric diversity across different categories of objects. While these objects may contain multiple parts, manipulating one part typically does not impact other parts’ state or joint limits, resulting in simplified manipulation mechanisms. Common actions in these environments include pushing or pulling a part, such as opening a drawer or pressing a button, which can be deduced purely from visual observation. However, real-world manipulation often depends on internal joint states that are not visible externally, necessitating adaptive manipulation policies based on feedback.

To better simulate real-world articulated object manipulation as well as corresponding mechanisms, we have identified five adaptive mechanisms that enhance the fidelity of our environment:

Lock Mechanism: Common in everyday objects like doors or safes, the lock mechanism requires an initial action such as rotating a key or knob or pressing a button to unlock the object before it can be opened. This mechanism tracks the key part’s joint state during manipulation and updates the lock state accordingly. If the lock state transitions to "unlock," the door joint limit is lifted to allow opening; otherwise, the door remains locked. Since the lock state cannot be inferred visually, the robot must interact with the object to determine the lock state and adapt its policy accordingly.

Random Rotation Direction: When rotating a knob, cap, or handle, the direction (*i.e.*, clockwise or counterclockwise) is determined by the internal revolute joint limit. Our environment randomly assigns the rotation direction upon initialization, preventing visual inference of the direction. The robot must attempt one direction and switch if unsuccessful.

Rotate & Slide Mechanism: This mechanism requires a part to be rotated to a specific angle before it can be lifted or pulled out, such as lifting the lid of a pressure cooker. The required rotation angle is not visually discernible, necessitating the robot to rotate the part incrementally and attempt to slide it to determine if the correct angle is reached. We randomize the revolute joint limit and initially set the prismatic joint limit to zero, lifting it once the correct angle is achieved.

Push/Rotate Mechanism: Due to the similar appearance of buttons and knobs, it is unclear whether a part should be pushed or rotated. For example, a lamp might be turned on by pushing a button in

216
217
218
219
220
221
222
223
224
225
226
227
228
229
230
231
232
233
234
235
236
237
238
239
240
241
242
243
244
245
246
247
248
249
250
251
252
253
254
255
256
257
258
259
260
261
262
263
264
265
266
267
268
269

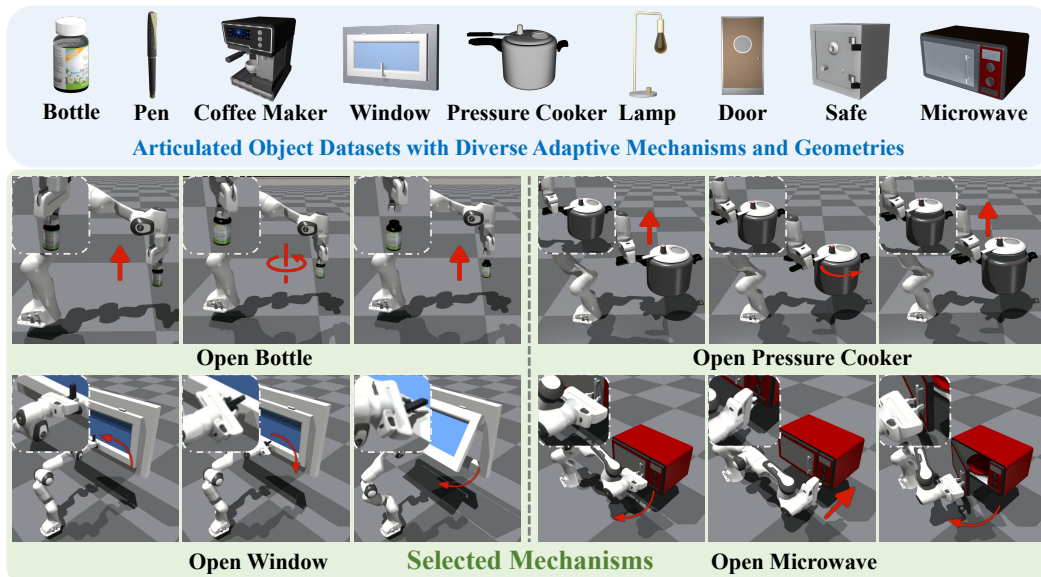


Figure 2: Adaptive manipulation dataset and environments. Bottle and Pressure Cooker feature the **Rotate & Slide** mechanism, requiring continued rotation after a failed lift. The window includes the **Lock** and **Random Rotation Direction** mechanisms, necessitating exploration of the correct rotation direction to unlock the latch. Microwave incorporates the **Lock** and **Switch Contact** mechanisms, where the robot must first pull the handle to check the lock state and press the button if locked.

some instances and rotating a knob in others. Our environment includes both revolute and prismatic joints for the same part in the URDF file and randomly determines whether the part should be pushed or rotated, adjusting the joint limit accordingly.

Switch Contact Mechanism: Based on the lock mechanism, this requires the robot to manipulate different key parts, such as a handle and a knob, if they are separate. For instance, in a safe, the robot must switch contact points during manipulation due to the lock state ambiguity, preventing it from determining the sequence of contact points at the outset.

Table 2 compares the richness and diversity of mechanisms between our environment and others. We selectively visualize the adaptive manipulation mechanisms of four categories in Figure 2. We defer details of the remaining categories to Appendix D.

4 METHOD

As illustrated in Figure 3, we propose a novel framework that learns an adaptive manipulation policy for various mechanisms from collected adaptive demonstrations. To achieve this, we leverage the annotated part poses in our dataset to generate expert manipulation trajectories in the environments, considering invisible internal states to ensure the trajectories are adaptive. Next, to model the expert trajectory distribution with high multi-modality, we employ 3D visual diffusion-based imitation learning (Ze et al., 2024; Chi et al., 2023), which learns the gradient of the action score function to generate actions.

4.1 ADAPTIVE DEMONSTRATION COLLECTION

Our goal is to generate adaptive demonstrations that are optimal under partial observation. For instance, when opening a microwave, the expert adaptive policy initially pulls the handle to check the lock state. If the latch is locked, the policy will push the button before opening the door. If the latch is not locked, the policy continues pulling the handle to open the door. In contrast, a static policy with full observation would know the lock state in advance and could directly open the door or push the button without first trying to pull the handle.

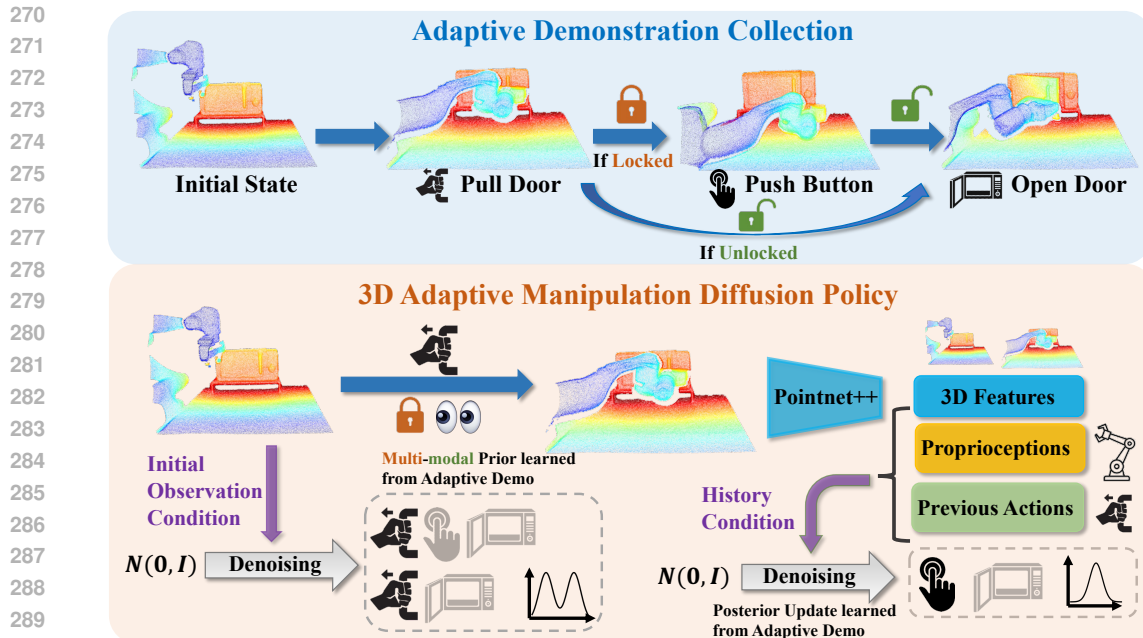


Figure 3: **Adaptive demonstration collection:** Given the uncertain lock state of a microwave, we instruct the robot to first pull the door to check if it is locked, and then follow two different trajectories based on the result. **Diffusion-based 3D adaptive manipulation policy:** Conditioning on the history of 3D visual features, proprioceptions, and actions, the policy denoises Gaussian noise into the trajectory distribution. Initially, the policy captures the bimodal distribution in the demonstration based on the initial observation. As the observed lock state is determined, the policy distribution adaptively shifts to a unimodal distribution.

We design rule-based expert adaptive policies to gather adaptive demonstrations in our simulation environments. We start by computing the bounding box of the part mesh and annotating the part pose through an interactive script. Using these annotations, we label the sequences of parts and manipulation actions for each category, ensuring optimal trajectories under partial observation. For example, the manipulation sequence for a locked safe is grasping the handle, pulling the door, grasping the knob, rotating the knob, grasping the handle, and opening the door. **Note that the recorded trajectories are end effector poses instead of the high-level action labels. More details are provided in Appendix C.** With these policies, we collect adaptive demonstrations of robot motion trajectories for all 9 categories of objects.

4.2 3D DIFFUSION-BASED ADAPTIVE POLICY LEARNING

Given the collected demonstration dataset $D = \{(o_t, a_t)\}$, we aim to learn a policy that models the conditional distribution $P(A_t|O_t, \hat{A}_t)$. Here A_t refers to the predicted action sequence $A_t = (a_t, \dots, a_{t+T_a})$, where T_a is the action horizon. O_t refers to the observation history, including 3D point clouds and proprioception states, $O_t = (o_{t-T_o}, \dots, o_t)$, where T_o is the history horizon. \hat{A}_t refers to action history, $\hat{A}_t = (a_{t-T_o-1}, \dots, a_{t-1})$.

However, conducting imitation learning on D is challenging due to its multi-modal nature: The ambiguity of the internal states of articulated objects results in multiple successful manipulation trajectories under the same visual observation. Thanks to recent progress in diffusion-based methods (Chi et al., 2023; Ze et al., 2024; Ke et al., 2024), we can better fit the multi-modal distribution by learning the action score function.

Following the Diffusion Policy (Chi et al., 2023), we utilize DDPM (Ho et al., 2020) to estimate the conditional distribution $P(A_t|O_t, \hat{A}_t)$. The DDPM scheduler performs K iterations of denoising steps to transform Gaussian noise A_t^K into a noise-free action A_t^0 . This process adheres to Eq. 1, where α_k , γ_k , and σ_k are parameters determined by the scheduler. This reverse process conditions the

action prediction on both observations and previous actions, differing from the vanilla implementation of the diffusion policy.

$$A_t^{k-1} = \alpha_k \left(A_t^k - \gamma_k \epsilon_\theta(A_t^k, O_t, \hat{A}_t, k) \right) + \mathcal{N}(0, \sigma_k^2 I) \quad (1)$$

The noise prediction network ϵ_θ is trained by minimizing the loss function in Eq. 2, which effectively minimizes the variational lower bound of the KL-divergence between the data distribution and the sample distribution drawn from DDPM:

$$\mathcal{L}(\theta) = \mathbb{E}_{\substack{k \sim \mathcal{U}(0,100), \\ \epsilon^k \sim \mathcal{N}(0, \sigma_k^2 I)}} \left[\left\| \epsilon^k - \epsilon_\theta(A_t^0 + \epsilon^k, O_t, \hat{A}_t, k) \right\|_2^2 \right] \quad (2)$$

In practice, the observation o_t consists of an observed third-view partial point cloud and the robot’s proprioception state (*e.g.*, end-effector pose, robot joint angles, and velocities). The point cloud is first cropped and downsampled by Farthest Point Sampling (FPS) and then encoded by PointNet++ (Qi et al., 2017). The action a_t is the next robot end-effector goal pose. Notably, we find that employing a 6D rotation representation (Ke et al., 2024) for the end-effector pose action stabilizes the training process. During execution, the policy only executes a sub-sequence of the predicted actions, as the adaptive manipulation process requires high-frequency adjustments.

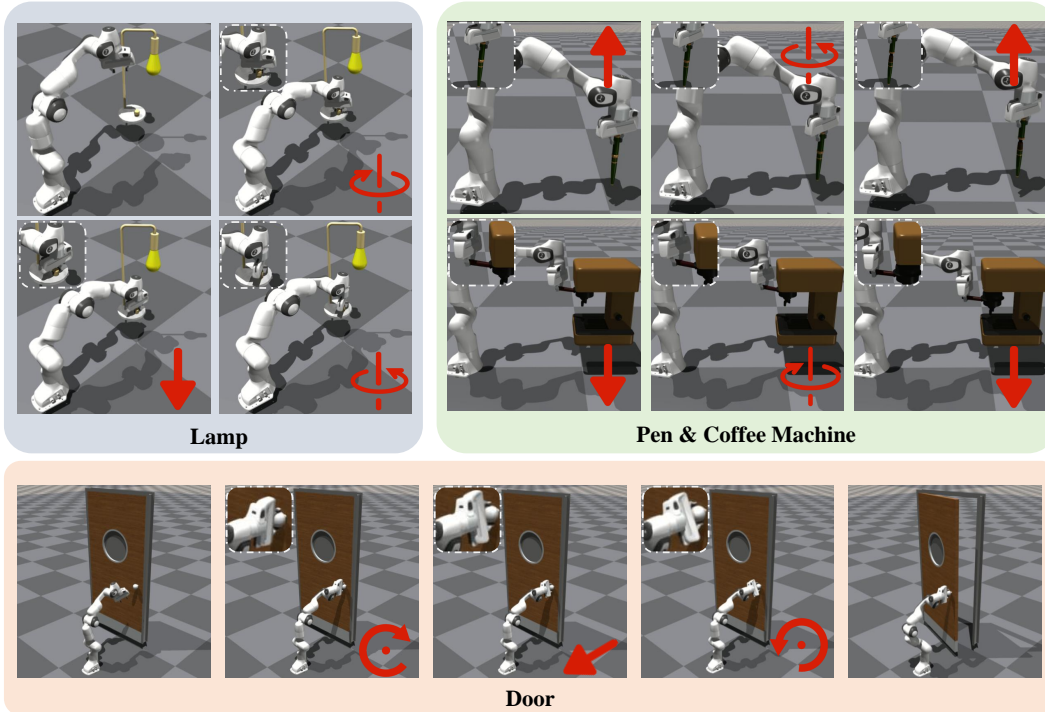


Figure 4: **Adaptive Environments and Qualitative Manipulation Results.** This figure shows the manipulation results of object categories apart from Figure 2.

5 EXPERIMENTS

5.1 SETTINGS AND METRIC

We conduct experiments in the category level covering all the 9 object categories, and collect 20 adaptive manipulation demonstrations for each object as the training data. For evaluation metric, we use success rate of manipulations. To evaluate what kind of adaptive demonstrations is the most beneficial to adaptive policy learning, we train adaptive policies on adaptive demonstrations with different numbers of adaptive trials.

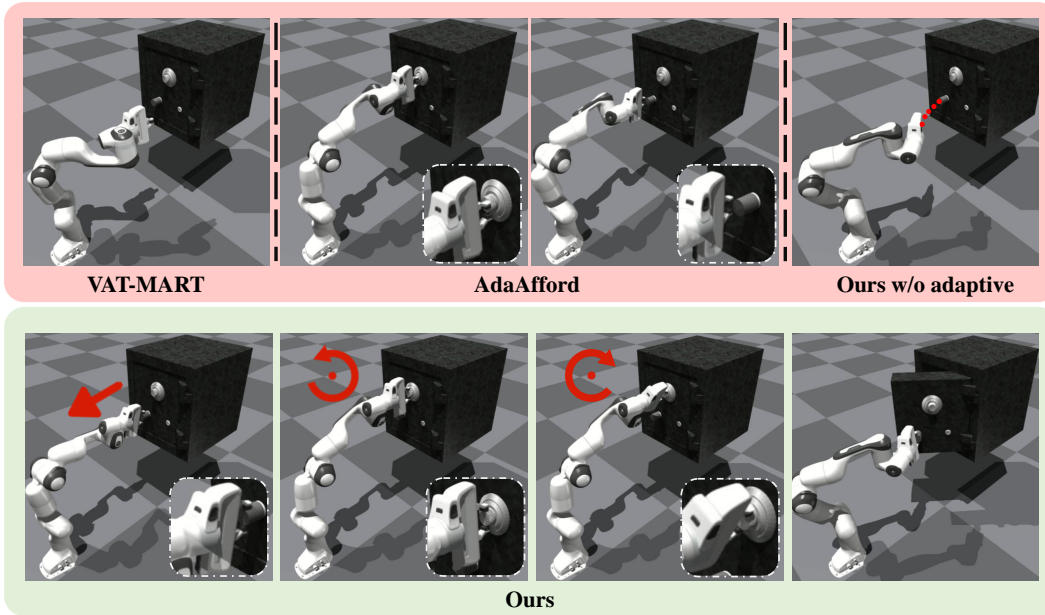











Figure 5: **Manipulation Trajectories Proposed by Our Method and Others.** Our method can sequentially propose stable and accurate adaptive actions, while others have their respective drawbacks.

Table 3: **Success Rates of Different Methods.** Our method outperforms baseline methods and the ablated version in all categories.

Method	Adaptive Manipulation								
									
VAT-MART	41.43±17.44	45.00±12.04	38.33±18.33	71.43±14.29	1.25±0.88	6.00±5.10	13.75±6.73	15.00±12.24	34.29±19.38
AdaAfford	42.86±14.29	70.00±11.83	55.00±15.00	61.43±22.18	21.25±16.31	77.00±17.35	45.00±17.85	21.25±11.25	52.86±18.13
Sampling	17.37±9.72	24.00±11.14	26.67±16.99	38.57±16.96	15.71±11.87	25.00±10.25	18.57±12.86	11.25±8.75	28.75±13.75
ACT	75.79±8.55	74.00±16.85	81.11±5.49	90.48±6.73	28.57±15.43	59.00±14.46	66.67±5.39	52.50±14.58	51.19±13.62
DP3	83.16±12.19	83.00±11.87	86.67±4.08	85.71±10.10	35.71±21.02	62.00±13.27	70.95±3.37	58.75±14.84	53.57±13.20
Ours w/o adaptive	87.14±14.91	80.00±10.00	85.00±8.90	91.42±11.42	38.75±20.50	58.00±38.16	74.77±2.81	56.25±13.98	54.29±20.00
Ours	95.07±9.70	99.05±0.81	98.33±4.99	97.14±5.71	61.25±33.28	100.00±0.0	94.33±2.38	88.75±10.38	82.53±14.72

5.2 BASELINES AND ABLATION

To demonstrate the superiority of our proposed method and its components in manipulating articulated objects with different mechanisms, we compare it with **state-of-the-art affordance-based methods, offline imitation learning methods, a sampling-based method, and an ablation of our method.**

- **VAT-Mart** (Wu et al., 2022), affordance-based (Zhao et al., 2022; Wu et al., 2023b) method that predicts the open-loop trajectories from the one-frame passive observation.
- **AdaAfford** (Wang et al., 2022), adaptive method that adjusts the manipulation policy based on history interactions using CVAE) (Sohn et al., 2015).
- **Sampling**, a planning-based method that samples a macro action from a discrete set at each high-level time step and then plans to the sub-goal pose associated with the selected macro action computed based on the object part pose annotation.
- **ACT** (Zhao et al., 2023), an imitation learning method that uses Action Chunking with Transformers and CVAE.
- **DP3** (Ze et al., 2024), Diffusion Policy extended with 3D visual representations.
- **Ours w/o adaptive**, replace the adaptive demonstration data with static demonstration data that is optimal under full observation, maintaining the diffusion-based imitation learning.

Table 4: **Effects of Repeated Adaptive Trials in Adaptive Demonstration for Bottle.** While adaptive trials are necessary for learning the adaptive policy, repeated adaptive trials make it more difficult to model the adaptive manipulation distribution.

Trials	0	1(ours)	2	3	4	5	6
Success Rate	0.8714	0.9364	0.7571	0.6571	0.5714	0.4143	0.4428

5.3 SIMULATION RESULTS

Table 3 and Figure 5 respectively show the success rates and manipulation trajectories of different methods. Figure 4 further shows more manipulation trajectories proposed by our method. Our method outperforms all other methods and demonstrates stable and accurate action trajectories for adaptive manipulation. From the visualizations, we can observe that, for **VAT-Mart**, as an open-loop method, it is difficult to fit the whole trajectory space and directly predict a manipulation trajectory at a time, and the open-loop method does not support adapting the policy from previously executed actions. Using the diffusion-based imitation method, our method can more accurately model the poses of actions using the limited number of data (such advantage is also demonstrated in other diffusion-based imitation studies (Chi et al., 2023; Ze et al., 2024)). **In contrast, AdaAfford suffers from the inferior multi-modal distribution modeling capability of CVAE and the increased training data requirements associated with point-level affordance learning. The Sampling-based method performs worse than AdaManip and other baselines because its sampling process because its sampling process cannot efficiently leverage priors or posteriors learned from demonstrations. While ACT and DP3 outperform affordance-based methods, they fall short of AdaManip due to the absence of an adaptive demonstration collection pipeline. Additionally, ACT is further limited by its lack of the robust multi-modality modeling capability provided by diffusion models.**

Ours w/o adaptive is not trained from demonstrations with recovery actions from failure trials, so the learned policy could not adapt from failure actions to finally achieve the goal. As illustrated in Figure 5, when the safe is locked and **Ours w/o adaptive** attempts to open the door, it fails to switch to rotating the knob and instead continues on the opening trajectory.

Table 4 shows the effects of repeated adaptive trials in adaptive demonstrations for training. When only using optimal successful actions (*i.e.*, 0 adaptive trials) under full observation, the model is the same with **Ours w/o adaptive** and could not have the adaptation capability. When using more than one adaptive trial at the same object state, these adaptive trials are redundant and increase the complexity of distributions to model, while not increasing the scenarios the policy can handle. Therefore, the performance decreases when the number of repeated adaptive trials increases from 1. These results validate our demonstration collection design, which limits the manipulation sequence to only one adaptive trial.

Table 5: Real-world Evaluation Results.

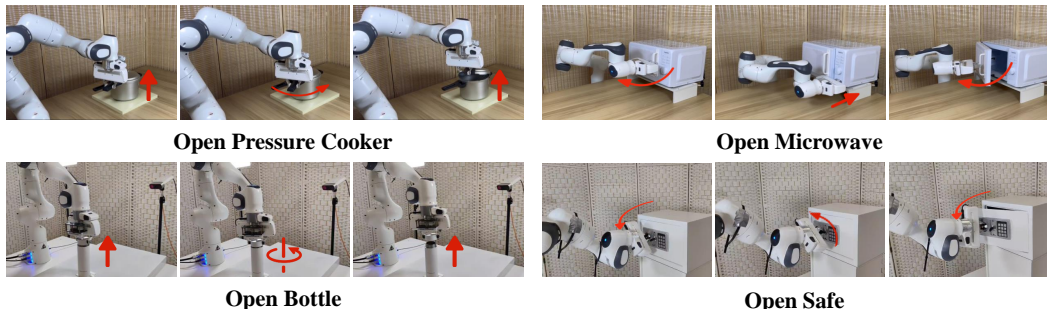
Tasks	Open Bottle	Open Microwave	Open Safe	Open Pressure Cooker
Success	8/10	7/10	5/10	5/10

5.4 REAL-WORLD EXPERIMENTS

To validate the generalization of our adaptive diffusion policy to real-world scenarios, we conduct experiments on various real-world objects like Pressure Cooker, Microwave, Bottle, and Safe. For the real-world settings, we employ a Franka Emika Panda Robot Arm as our agent. To capture 3d visual observation, we position an Azure Kinect DK camera adjacent to the robot arm. Our policy takes the real-time point clouds from the depth camera, the robot state from the robot arm, and previous actions as the input, and generates the corresponding end-effector action in a close-loop fashion. We collected 35 adaptive expert demonstrations for each object **by human teleoperation** to train the policies, and conducted 10 evaluation trials per object.

Table 5 presents the number of successful executions across four real-world tasks. The results in Figure 6 demonstrate that our adaptive policy can be effectively applied to real-world scenarios. To

486 better illustrate this adaptive behavior, we visualize different trajectories under different object states
 487 in Figure 7. The red trajectory shows that the robot finds out that the microwave is locked after it
 488 failed to pull the door and turned to push the button to unlock the door. Conversely, if the microwave
 489 is initially unlocked, the robot will continue to open the door after it grasps the handle, as depicted by
 490 the blue trajectory in sub-figure 2 of Figure 7. For more visualizations, please see Appendix D.



491
492
493
494
495
496
497
498
499
500
501
502
503
504
505
506
507
508
509
510
511
512
513
514
515
516
517
518
519
520
521
522
523
524
525
526
527
528
529
530
531
532
533
534
535
536
537
538
539

Figure 6: Manipulation Trajectories of Real-World Scenarios.

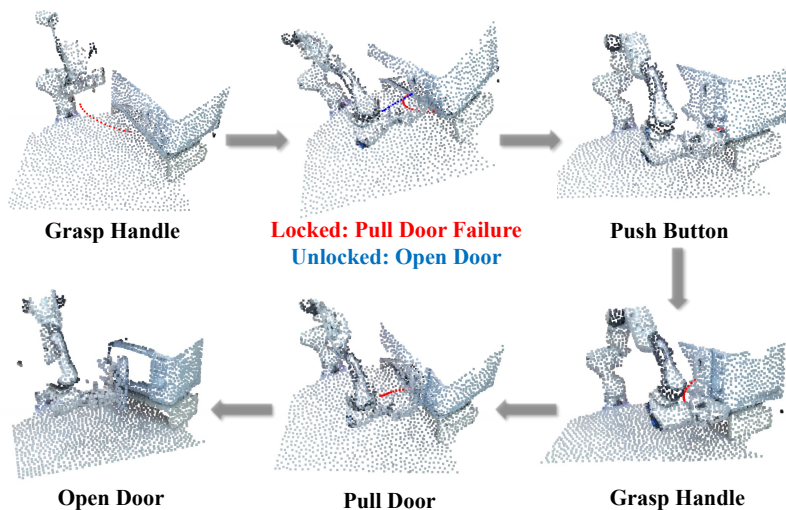


Figure 7: Visualization of adaptive policy of Open Microwave in the real world. The trajectories vary depending on the state of the microwave. The red trajectory represents the executed trajectory when the microwave is locked. In subfigure 2, the blue trajectory illustrates the robot’s action when the microwave is unlocked, prompting it to continue opening the door. The red trajectory shows that the robot failed to pull the locked door and turned to push the button.

6 CONCLUSION

We study the problem of adaptive manipulation policy for manipulating articulated objects with diverse and complex mechanisms, build environments with different categories of such objects that support the various manipulation mechanisms, and propose a novel framework that learns the adaptive manipulation policy for various mechanisms from diverse adaptive demonstrations based on diffusion policy. The significance of our proposed environment and the effectiveness of the proposed adaptive policy learning framework have been demonstrated by our experiments.

Our paper represents the initial study into the environment suitable for adaptive manipulation policy learning. Currently, our dataset encompasses 9 categories with a total of 277 objects, which we plan to expand by introducing more categories and instances to cover increasingly complex and realistic mechanisms. Additionally, incorporating deformable object manipulation into adaptive tasks represents a significant direction for future research. Moving forward, the AdaManip environment will progressively include a broader spectrum of real adaptive manipulation tasks, making it a comprehensive platform for both training and testing adaptive manipulation policies.

540
541
542
543
544
545
546
547
548
549
550
551
552
553
554
555
556
557
558
559
560
561
562
563
564
565
566
567
568
569
570
571
572
573
574
575
576
577
578
579
580
581
582
583
584
585
586
587
588
589
590
591
592
593

REFERENCES

- Angel X. Chang, Thomas A. Funkhouser, Leonidas J. Guibas, Pat Hanrahan, Qi-Xing Huang, Zimo Li, Silvio Savarese, Manolis Savva, Shuran Song, Hao Su, Jianxiong Xiao, L. Yi, and Fisher Yu. Shapenet: An information-rich 3d model repository. *ArXiv*, abs/1512.03012, 2015. URL <https://api.semanticscholar.org/CorpusID:2554264>.
- Cheng Chi, Siyuan Feng, Yilun Du, Zhenjia Xu, Eric A. Cousineau, Benjamin Burchfiel, and Shuran Song. Diffusion policy: Visuomotor policy learning via action diffusion. *ArXiv*, abs/2303.04137, 2023. URL <https://api.semanticscholar.org/CorpusID:257378658>.
- Yushi Du, Ruihai Wu, Yan Shen, and Hao Dong. Learning part motion of articulated objects using spatially continuous neural implicit representations. In *British Machine Vision Conference (BMVC)*, November 2023.
- Ben Eisner, Harry Zhang, and David Held. Flowbot3d: Learning 3d articulation flow to manipulate articulated objects. *arXiv preprint arXiv:2205.04382*, 2022.
- Haoran Geng, Ziming Li, Yiran Geng, Jiayi Chen, Hao Dong, and He Wang. Partmanip: Learning cross-category generalizable part manipulation policy from point cloud observations. In *Proceedings of the IEEE/CVF Conference on Computer Vision and Pattern Recognition*, pp. 2978–2988, 2023a.
- Haoran Geng, Helin Xu, Chengyang Zhao, Chao Xu, Li Yi, Siyuan Huang, and He Wang. Gapartnet: Cross-category domain-generalizable object perception and manipulation via generalizable and actionable parts. In *Proceedings of the IEEE/CVF Conference on Computer Vision and Pattern Recognition*, pp. 7081–7091, 2023b.
- Yiran Geng, Boshi An, Haoran Geng, Yuanpei Chen, Yaodong Yang, and Hao Dong. End-to-end affordance learning for robotic manipulation. *ICRA*, 2023c.
- Ran Gong, Jiangyong Huang, Yizhou Zhao, Haoran Geng, Xiaofeng Gao, Qingyang Wu, Wensi Ai, Ziheng Zhou, Demetri Terzopoulos, Song-Chun Zhu, et al. Arnold: A benchmark for language-grounded task learning with continuous states in realistic 3d scenes. In *Proceedings of the IEEE/CVF International Conference on Computer Vision (ICCV)*, 2023.
- Jiayuan Gu, Fanbo Xiang, Xuanlin Li, Zhan Ling, Xiqiang Liu, Tongzhou Mu, Yihe Tang, Stone Tao, Xinyue Wei, Yunchao Yao, et al. Maniskill2: A unified benchmark for generalizable manipulation skills. *arXiv preprint arXiv:2302.04659*, 2023.
- Nick Heppert, Muhammad Zubair Irshad, Sergey Zakharov, Katherine Liu, Rares Andrei Ambrus, Jeannette Bohg, Abhinav Valada, and Thomas Kollar. Carto: Category and joint agnostic reconstruction of articulated objects. In *Proceedings of the IEEE/CVF Conference on Computer Vision and Pattern Recognition*, pp. 21201–21210, 2023.
- Jonathan Ho, Ajay Jain, and Pieter Abbeel. Denoising diffusion probabilistic models. *Advances in neural information processing systems*, 33:6840–6851, 2020.
- Tsung-Wei Ke, Nikolaos Gkanatsios, and Katerina Fragkiadaki. 3d diffuser actor: Policy diffusion with 3d scene representations. *arXiv preprint arXiv:2402.10885*, 2024.
- Jiahui Lei, Congyue Deng, William B Shen, Leonidas J Guibas, and Kostas Daniilidis. Nap: Neural 3d articulated object prior. *Advances in Neural Information Processing Systems*, 36, 2024.
- Yu Li, Kai Cheng, Ruihai Wu, Yan Shen, Kaichen Zhou, and Hao Dong. Mobileafford: Mobile robotic manipulation through differentiable affordance learning. In *2nd Workshop on Mobile Manipulation and Embodied Intelligence at ICRA 2024*, 2024a. URL <https://openreview.net/forum?id=f6sc69sfrL>.
- Yu Li, Xiaojie Zhang, Ruihai Wu, Zilong Zhang, Yiran Geng, Hao Dong, and Zhaofeng He. Unidoormanip: Learning universal door manipulation policy over large-scale and diverse door manipulation environments. *arXiv preprint arXiv:2403.02604*, 2024b.

594 Suhan Ling, Yian Wang, Shiguang Wu, Yuzheng Zhuang, Tianyi Xu, Yu Li, Chang Liu, and Hao
595 Dong. Articulated object manipulation with coarse-to-fine affordance for mitigating the effect of
596 point cloud noise. *ICRA*, 2024.

597

598 Liu Liu, Wenqiang Xu, Haoyuan Fu, Sucheng Qian, Qiaojun Yu, Yang Han, and Cewu Lu. Akb-48:
599 A real-world articulated object knowledge base. In *Proceedings of the IEEE/CVF Conference on*
600 *Computer Vision and Pattern Recognition*, pp. 14809–14818, 2022.

601

602 Viktor Makoviychuk, Lukasz Wawrzyniak, Yunrong Guo, Michelle Lu, Kier Storey, Miles Macklin,
603 David Hoeller, Nikita Rudin, Arthur Allshire, Ankur Handa, et al. Isaac gym: High performance
604 gpu-based physics simulation for robot learning. *arXiv preprint arXiv:2108.10470*, 2021.

605

606 Kaichun Mo, Shilin Zhu, Angel X. Chang, Li Yi, Subarna Tripathi, Leonidas J. Guibas, and Hao
607 Su. PartNet: A large-scale benchmark for fine-grained and hierarchical part-level 3D object
608 understanding. In *The IEEE Conference on Computer Vision and Pattern Recognition (CVPR)*,
609 June 2019.

610

611 Kaichun Mo, Leonidas J. Guibas, Mustafa Mukadam, Abhinav Gupta, and Shubham Tulsiani.
612 Where2act: From pixels to actions for articulated 3d objects. In *Proceedings of the IEEE/CVF*
613 *International Conference on Computer Vision (ICCV)*, pp. 6813–6823, October 2021.

614

615 Tongzhou Mu, Zhan Ling, Fanbo Xiang, Derek Cathera Yang, Xuanlin Li, Stone Tao, Zhiao Huang,
616 Zhiwei Jia, and Hao Su. Maniskill: Generalizable manipulation skill benchmark with large-scale
617 demonstrations. In *Thirty-fifth Conference on Neural Information Processing Systems Datasets*
618 *and Benchmarks Track (Round 2)*, 2021.

619

620 Chuanruo Ning, Ruihai Wu, Haoran Lu, Kaichun Mo, and Hao Dong. Where2explore: Few-shot
621 affordance learning for unseen novel categories of articulated objects. In *Advances in Neural*
622 *Information Processing Systems (NeurIPS)*, 2023.

623

624 Charles Ruizhongtai Qi, Li Yi, Hao Su, and Leonidas J Guibas. Pointnet++: Deep hierarchical feature
625 learning on point sets in a metric space. *Advances in neural information processing systems*, 30,
626 2017.

627

628 Kihyuk Sohn, Honglak Lee, and Xinchen Yan. Learning structured output representation using deep
629 conditional generative models. *Advances in neural information processing systems*, 28, 2015.

630

631 Trimble. 3dwarehouse. <https://3dwarehouse.sketchup.com/>.

632

633 Yusuke Urakami, Alec Hodgkinson, Casey Carlin, Randall Leu, Luca Rigazio, and Pieter
634 Abbeel. Doorgym: A scalable door opening environment and baseline agent. *arXiv preprint*
635 *arXiv:1908.01887*, 2019.

636

637 Yian Wang, Ruihai Wu, Kaichun Mo, Jiaqi Ke, Qingnan Fan, Leonidas Guibas, and Hao Dong.
638 Adaafford: Learning to adapt manipulation affordance for 3d articulated objects via few-shot
639 interactions. *European conference on computer vision (ECCV 2022)*, 2022.

640

641 Fangyin Wei, Rohan Chabra, Lingni Ma, Christoph Lassner, Michael Zollhöfer, Szymon
642 Rusinkiewicz, Chris Sweeney, Richard Newcombe, and Mira Slavcheva. Self-supervised neural ar-
643 ticulated shape and appearance models. In *Proceedings of the IEEE/CVF Conference on Computer*
644 *Vision and Pattern Recognition*, pp. 15816–15826, 2022.

645

646 Ruihai Wu, Yan Zhao, Kaichun Mo, Zizheng Guo, Yian Wang, Tianhao Wu, Qingnan Fan, Xuelin
647 Chen, Leonidas Guibas, and Hao Dong. VAT-mart: Learning visual action trajectory proposals for
manipulating 3d ARTiculated objects. In *International Conference on Learning Representations*,
2022. URL <https://openreview.net/forum?id=iEx3PiooLy>.

648

649 Ruihai Wu, Kai Cheng, Yan Zhao, Chuanruo Ning, Guanqi Zhan, and Hao Dong. Learning
650 environment-aware affordance for 3d articulated object manipulation under occlusions. In
651 *Thirty-seventh Conference on Neural Information Processing Systems*, 2023a. URL <https://openreview.net/forum?id=Re2NHyoZ5l>.

648 Ruihai Wu, Chuanruo Ning, and Hao Dong. Learning foresightful dense visual affordance for
649 deformable object manipulation. In *IEEE International Conference on Computer Vision (ICCV)*,
650 2023b.

651 Fanbo Xiang, Yuzhe Qin, Kaichun Mo, Yikuan Xia, Hao Zhu, Fangchen Liu, Minghua Liu, Hanxiao
652 Jiang, Yifu Yuan, He Wang, et al. Sapien: A simulated part-based interactive environment.
653 In *Proceedings of the IEEE/CVF Conference on Computer Vision and Pattern Recognition*, pp.
654 11097–11107, 2020.

655 Ran Xu, Yan Shen, Xiaoqi Li, Ruihai Wu, and Hao Dong. Naturalvlm: Leveraging fine-grained
656 natural language for affordance-guided visual manipulation. *arXiv preprint arXiv:2403.08355*,
657 2024.

658 Zhenjia Xu, He Zhanpeng, and Shuran Song. Umpnet: Universal manipulation policy network for
659 articulated objects. *IEEE Robotics and Automation Letters*, 2022.

660 Ge Yan, Yueh-Hua Wu, and Xiaolong Wang. Dnact: Diffusion guided multi-task 3d policy learning.
661 *arXiv preprint arXiv:2403.04115*, 2024.

662 Yanjie Ze, Gu Zhang, Kangning Zhang, Chenyuan Hu, Muhan Wang, and Huazhe Xu. 3d diffu-
663 sion policy. *ArXiv*, abs/2403.03954, 2024. URL [https://api.semanticscholar.org/
664 CorpusID:268253298](https://api.semanticscholar.org/CorpusID:268253298).

665 Harry Zhang, Ben Eisner, and David Held. Flowbot++: Learning generalized articulated objects
666 manipulation via articulation projection. *arXiv preprint arXiv:2306.12893*, 2023.

667 Tony Z Zhao, Vikash Kumar, Sergey Levine, and Chelsea Finn. Learning fine-grained bimanual
668 manipulation with low-cost hardware. *arXiv preprint arXiv:2304.13705*, 2023.

669 Yan Zhao, Ruihai Wu, Zhehuan Chen, Yourong Zhang, Qingnan Fan, Kaichun Mo, and Hao Dong.
670 Dualafford: Learning collaborative visual affordance for dual-gripper object manipulation. *arXiv
671 preprint arXiv:2207.01971*, 2022.

672
673
674
675
676
677
678
679
680
681
682
683
684
685
686
687
688
689
690
691
692
693
694
695
696
697
698
699
700
701

702
703
704
705
706
707
708
709
710
711
712
713
714
715
716
717
718
719
720
721
722
723
724
725
726
727
728
729
730
731
732
733
734
735
736
737
738
739
740
741
742
743
744
745
746
747
748
749
750
751
752
753
754
755

Table 6: **Parameters for training and diffusion model**

Training	Values
Hardware Configuration	NVIDIA GeForce GTX 4090
Weight Decay	1e-6
Batch Size	64
Optimizer	Adam
Learning Rate	1e-4
Epochs	500
Time Expense	3h
Model	Values
Pointcloud Size	4096
Backbone	Unet
Observation History Horizon	4
Prediction Horizon	4
Action Horizon	2
EMAModel	True
Diffusion Timestep	100
Noise Scheduler	squaredcos
Action Space	absolute end-effector pose

A HYPER-PARAMETERS FOR EXPERIMENTS

Table 6 summarizes the hyperparameters for our diffusion policy model and training details.

B DATASET CONSTRUCTION

Apart from object assets collected from existing datasets (Xiang et al., 2020; Li et al., 2024b), most of the object assets in our dataset are obtained from 3Dwarehouse (Trimble). We dedicate significant time and effort to carefully selecting the available object meshes, segmenting them into distinct parts, re-aligning the object mesh coordinate systems, and subsequently developing Python scripts to facilitate the efficient synthesis of operational dataset instances. Similar to GPartNet (Geng et al., 2023b), we annotate the object assets with rich and comprehensive labels.

C DETAILED EXPERT POLICY DESIGN FOR ADAPTIVE DEMONSTRATION COLLECTION

C.1 POSE ANNOTATION

To achieve precise part operation, we employ a pose labeling approach for the parts. Initially, we roughly estimate the part pose through the bounding box of the part mesh calculated using the Python library trimesh. Subsequently, we observe the pose annotation results in real-time through an online interactive script to complete the precise annotation of the pose.

C.2 ADAPTIVE MANIPULATION SEQUENCE

Bottle Rotate Cap after a failed Lift Up. Randomly sample Rotate/Lift if the previous action is Rotate.

Pen Same as Bottle.

Pressure Cooker Rotate Handle after a failed Lift Up. Randomly sample Rotate/Lift if the previous action is Rotate.

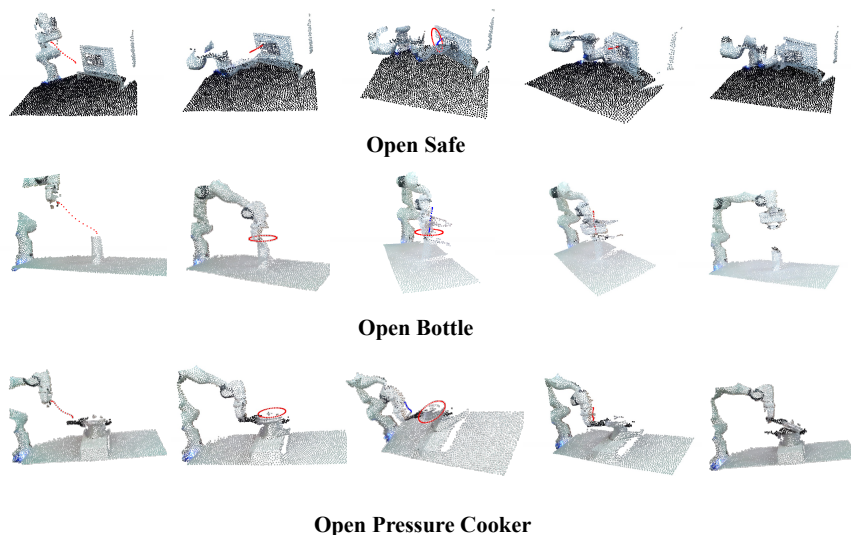
Coffee Maker Rotate Portafilter after a failed Pull Down. Randomly sample Rotate/Pull if the previous action is Rotate.

756 **Window** Randomly choose a direction to Rotate Handle. If failed, choose the other direction. Rotate
 757 Handle after a failed open trial. Randomly sample Rotate/Open if the previous action is Rotate.
 758
 759 **Door** Same as Window.
 760 **Lamp** Randomly choose to Push/Clockwise Rotate/Counter Clockwise Rotate. Never choose a failed
 761 action.
 762 **Safe** Pull Door. If succeed, then continue opening the door. If failed, Rotate Knob. Randomly choose
 763 a direction to Rotate and choose the other one if failed. Then Pull Door again to open it.
 764
 765 **Microwave** Pull Door. If succeed, then continue opening the door. If failed, Push Button. Then Pull
 766 Door again to open it.

767 C.3 TRAJECTORY SPARSIFICATION

769 If the history consists of a dense trajectory of the robot's end effector poses, the policy would require
 770 a long history context length to capture previous failures. However, training a policy with a long
 771 history context is challenging, as it requires more computing resources and is less robust. To mitigate
 772 this issue, we chose to sparsify the trajectory. Only key frames of the demonstration trajectories
 773 are saved for imitation learning, but the recorded actions are still 6D end effector poses instead of
 774 high-level macro actions.

775 For example, in the open-safe task, the recorded history includes grasping poses and several ma-
 776 nipulation poses while omitting most intermediate steps. The history condition for the policy is as
 777 follows: [grasp the handle, pull the door and fail to open]. Other intermediate poses during execution
 778 are excluded from the history. Based on this context, the robot predicts the next goal pose [unlock the
 779 key]. Once the goal pose is predicted, we apply inverse kinematics (IK) to plan the path for execution.
 780



801 Figure 8: Visualization of Open Safe/Bottle/Pressure Cooker Experiment in the real world. The red
 802 trajectory represents the executed trajectory. The blue trajectory indicates the actions under other
 803 object states.

804 D MECHANISM VISUALIZATION AND EXPERIMENTAL RESULTS

805
 806 Figure 4 illustrates the operating mechanism of the remaining categories and the experimental results.
 807 The mechanism of the lamp in the upper left corner is "**Push/Rotate**", which can be operated by
 808 pressing/rotating the button/knob, but only one way is correct. The pen and coffee machine in the
 809

810 upper right corner fall under the "**Rotate/Slide**". To operate them, you need to rotate a specific part
811 to a certain angle to open the pen cap or the coffee machine handle. The door at the bottom belongs to
812 the "**Random Rotation Direction**" and "**Lock**", where the handle must be rotated either clockwise
813 or counterclockwise to open the door.

814 Figure 8 shows the visualizations of the other 3 experiments in real world apart from Open Microwave
815 shown in Figure 7. In these visualizations, the red trajectories represent the paths actually executed
816 by the robot, while the blue trajectories indicate potential paths under different object states. For
817 instance, in Sub-figure 3 of the Open Bottle experiment, the blue trajectory shows that if the cap is
818 rotated sufficiently, the robot can then lift the cap. This visualization helps illustrate the adaptability
819 of the robot's actions based on the observed state of the objects involved.
820

821
822
823
824
825
826
827
828
829
830
831
832
833
834
835
836
837
838
839
840
841
842
843
844
845
846
847
848
849
850
851
852
853
854
855
856
857
858
859
860
861
862
863